Superconductivity 3 (2022) 100024

Contents lists available at ScienceDirect

Superconductivity

journal homepage: www.elsevier.com/locate/supcon

Optimizing coil configurations for AC loss reduction in REBCO HTS fast-ramping magnets at cryogenic temperatures

Zhenan Jiang [a,*], Honghai Song [b,*], Wenjuan Song [c], Rodney A. Badcock [a]

[a] Robinson Research Institute, Victoria University of Wellington, Wellington, New Zealand
[b] Department of Physics and Astronomy, State University of New York at Stony Brook, New York, USA
[c] James Watts School of Engineering, University of Glasgow, Glasgow, UK

ARTICLE INFO

Keywords:
Fast ramping magnet
AC loss reduction
H-formulation
REBCO
Flux diverters

ABSTRACT

AC loss is one of the critical issues for designing REBCO fast-ramping magnets operating at cryogenic temperatures. There are many ways to reduce AC loss for coil windings. However, it is not clear which method is the most effective way to minimize AC loss in the coil windings for a given Ampere-turns. In this work, we numerically studied coil configurations of several small superconducting magnets constructed from 12 mm SuperPower REBCO coated conductors, for fast-ramping application with the same Ampere-turns to identify the lowest AC loss among them. The HTS magnets have a total turn number of 50 and inner diameter of 30 cm, carrying AC current operating in the temperature range of 20–40 K at 25 Hz. We incorporated several existing loss reduction strategies including spacing between the turns for single pancake coils, grading I_c values for the solenoid configuration, and applying flux diverters to shape the magnetic field around the coil windings. The simulation was implemented using a homogenized *H*-formulation. Across all studied loss reduction methods, the use of flux diverters has the largest impact in AC loss reduction. The AC loss values in the solenoid winding comprising a stack of five single pancake coils with 0.1 mm turn-to-turn gap with the flux diverters agree well with those in the single pancake coil for 2 mm turn-to-turn gap with the flux diverters. Solenoid type coil configurations with flux diverters generate much smaller AC loss than the single pancake type with flux diverters when they generate the same center magnetic field.

1. Introduction

Remarkable progress has been made in the properties of commercial REBCO (where RE stands for rare-earth, B is for barium, C is for copper and O is for Oxygen) superconductor. New flux pinning doping has led to high I_c and long-length production is routine. High quality commercial REBCO conductors are being pursued by nearly a dozen commercial manufacturers globally and there have been many successful demonstrations in the field of power application [1–3] and high field magnets [4–7]. A unique, but little studied, application of HTS is for fast ramping magnets [8], particularly at a frequency of ~ 25 Hz and with high current up to a few hundred Amps [9,10]. Owing to its high critical temperature (T_c), REBCO based fast ramping magnets can be designed and operated at temperatures ranging from 20 K to 40 K to fully utilise the high current – carrying capacity [11].

Operating at higher temperatures than 4.2 K allows GM or Pulse tube cryocoolers to be viable options for conduction-cooling. Conduction cooled magnets are becoming more attractive since the appearance of the global Helium shortage since early 2022 [12,13]. Some unique applications, these HTS magnets are required to operate at a specific frequency [14,15]. Unlike traditional DC superconducting magnets, which only consider AC loss during ramping up and down, AC loss exists all the time. If the AC loss in the coil windings is greater than hundreds of watts [16], it will cause serious issues for the cooling system and hence measures have to be taken to reduce AC loss for the fast-ramping application.

One of many methods to reduce AC loss in the coil windings is to wind the coil windings using low-loss-conductors [17–19]. The use of multifilamentary coated conductors to assemble CORC cables are a promising candidate for low-loss coil windings. The AC loss under perpendicular AC magnetic fields can be effectively reduced due to the combination of their fine filamentary structure and the spiral shape of the strands which is equivalent to twisting [20–23]. A potential drawback with CORC cables could be a lower engineering current density due to the round core and hence they are not suitable for compact coil windings.

* Corresponding authors.
E-mail addresses: Zhenan.Jiang@vuw.ac.nz (Z. Jiang), Honghai.Song@stonybrook.edu (H. Song).

https://doi.org/10.1016/j.supcon.2022.100024
Received 27 July 2022; Revised 31 August 2022; Accepted 31 August 2022
Available online 7 September 2022

An alternate technique to reduce AC loss in coil windings is to reduce the magnetic interactions between coil turns or manipulate the magnetic field around the coils to favour lower AC loss in the coil windings. There are many ways to reduce AC loss for coil windings: spacing between coil turns for single pancake coils (SPC) [24]; hybrid coil winding structure where high I_c wires are used in the end part of the windings and low I_c wires are used in the central part of the windings [25,26]; positioning magnetic flux diverters at the end of the coils to reduce the perpendicular magnetic field components to the conductor wide-face [27–32]. However, it is not clear which method is the most effective way to minimize AC loss in the coil windings for a given Ampere-turns *NI,* where *N* is the number of coil turns and *I* is the coil current.

In this work, we try to numerically obtain an optimized configuration among several small fast-ramping HTS magnet designs with the same Ampere-turns which gives the smallest AC loss using all the loss reduction methodologies mentioned above. The base specifications of the design are listed in Table 1. The HTS magnets have a total turn number of 50 and inner diameter of 30 cm, carrying AC current operating in the temperature range of 20–40 K. The frequency of the AC current is set at 25 Hz. The following are the coil configurations considered in this work:

a) SPCs with g_h = 0.1 mm, 1 mm, and 2 mm, where g_h is horizontal gap between turns, as shown in Fig. 1(a).
b) 5PC (a stack of five SPCs) with g_v = 2 mm, g_h = 0.1 mm, 1 mm, and 2 mm, where g_v is the vertical gap between the turns. Each SPC composing the 5PCs has 10 turns, as shown in Fig. 1(b)
c) 5PC_HBs: The 5PC has hybrid coil structure (Fig. 1(b)), where two end windings (green) have different I_c values compared with the center winding (blue).
d) SPCs and 5PC_HBs with flux diverters. A SPC with and without flux diverters is illustrated in Fig. 2.

The simulated AC loss values in the HTS magnets are compared. The magnetic field distribution around the coil windings, and current density in the coil windings, are compared to understand the impact on AC loss with configuration. In most magnet applications, it is useful to compare AC loss in coil windings for similar bore magnetic fields. It is important to note that the above designs have the same ampere-turns but generate slightly different bore magnetic field due the small geometric differences. Magnetic field distributions along the central axis (*z*-axis) in the different configurations are compared when they generate 0.15 T at the center point. AC loss values in the magnets are compared at the same center bore fields.

2. Numerical method

Numerical calculation for the HTS magnet was carried out in a 2D axisymmetric model using commercial software COMSOL Multiphysics, using *H* formulation [33] and homogenization method [34]. The numerical method was validated in our previous works on a 1-MVA HTS transformer [26,30]. The same modelling method was adopted to analyse the magnet and calculate the AC losses in this work. Fig. 3 shows the cross-section of the 2D axisymmetric model

Table 1
REBCO coil specification for AC loss reduction.

Coil parameter (unit)	Value
ID (mm)	**300**
OD (mm)	Depending on turn gaps
Total turn number, *N*	**50**
Peak coil current (A)	$I_{t,\ coil}$
Ampere-turns, *NI*	**50*** $I_{t,\ coil}$

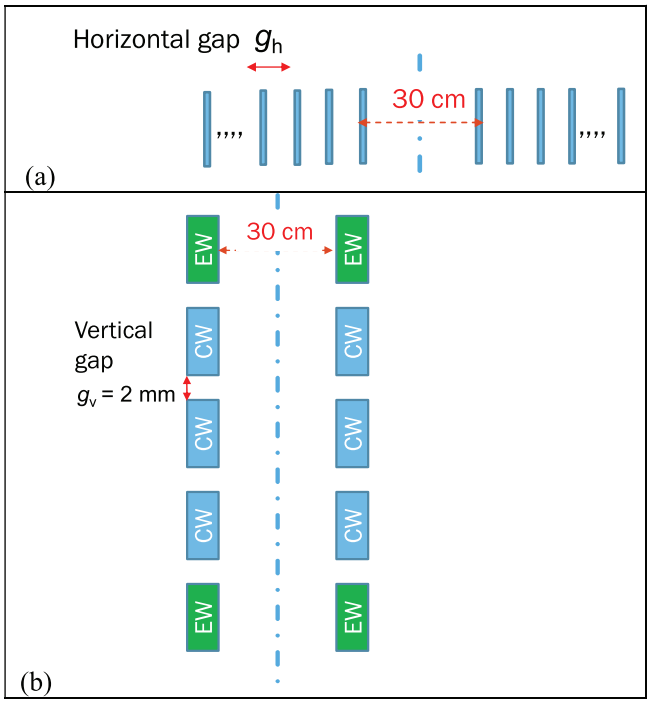

Fig. 1. Two main configurations in AC loss reduction. In the upper schematic, horizontal gap between turns are 0.1 mm, 1 mm, and 2 mm respectively. In the lower one, vertical gap stays at 2 mm, but the horizontal gaps between turns are 0.1 mm, 1 mm, and 2 mm respectively. The hybrid winding means that the conductors in the end winding (EW) and center winding (CW) have different critical currents, other than uniform critical current, as indicated in green and blue color.

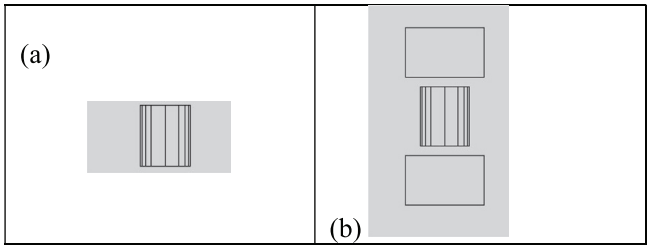

Fig. 2. Flux divertors are added to top and bottom of the winding pack (co-axis with the coil and in a ring shape). It intends to realign the flux direction, so that the flux parallel to the conductor surface at the magnet top and bottom edges.

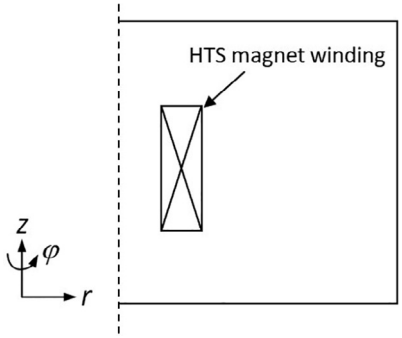

Fig. 3. Schematic of the 2D axisymmetric model for a HTS magnet winding.

for a HTS winding and the specifications of the REBCO wire considered in this work is shown in Table 2.

Radial and axial magnetic field components $H = [H_r, H_z]$ are the variables computed directly in the model. Current I flows in the φ direction, and local electric field E_φ and current density J_φ in the coil are expressed as,

$$E_\varphi = \rho J_\varphi \tag{1}$$

where ρ is the resistivity of the material. In the air domain, ρ is treated as a constant, 1 Ω/m [35]; while in superconducting domain, ρ is derived from the E-J power law, and it is expressed in Equation (2),

$$\rho = \frac{E_\varphi}{J_\varphi} = E_c \left|\frac{J_\varphi}{J_c(B)}\right|^{n-1} \frac{1}{J_c(B)} \tag{2}$$

where power index $n = 25$, $E_c = 10^{-4}$ V/m; $J_c(B)$ is the critical current density dependence on external magnetic field, derived from the measured $I_c(B)$ data[26]; S is the cross-section of the conductor. A modified Kim model [35] for the $J_c(B)$ curve is used in the model,

$$J_c(B) = I_{c0}\left(1 + \frac{k^2 B_{//}^{\ 2} + B_\perp^{\ 2}}{B_0^{\ 2}}\right)^{-\alpha} / S \tag{3}$$

where B_0, k and α are fitting parameters by comparing with the measured $I_c(B)$ results. In this case, $B_\perp$ is the radial magnetic field B_r and $B_{||}$ is the axial magnetic field B_z. The measured $I_c(B)$ results of the superconductor at 20 K, 30 K and 40 K are shown in Fig. 4. B_0, k and α of the REBCO wire at 20 K, 30 K and 40 K were obtained by fitting the experimental results in Fig. 4 and were listed in Table 3.

The current density in φ direction along conductor length is derived from the Ampere's law,

$$\boldsymbol{J}_\varphi = \frac{\partial H_r}{\partial z} - \frac{\partial H_z}{\partial r} \tag{4}$$

Faraday's law is written as,

$$\nabla \times \mathbf{E} = -\frac{\partial \boldsymbol{B}}{\partial t} = -\mu_0 \mu_{re} \frac{\partial \mathbf{H}}{\partial t} \tag{5}$$

where μ_0 is free-space magnetic permeability and $\mu_{re} = 1$ is the relative magnetic permeability in the model.

The governing equation is derived from the (1)–(5), which can be expressed as,

$$\begin{cases} \mu_0 \mu_{re} \frac{\partial H_r}{\partial t} - \frac{1}{r} \frac{\partial \left(r\rho\left(\frac{\partial H_r}{\partial z} - \frac{\partial H_z}{\partial r}\right)\right)}{\partial z} = 0 \\ \mu_0 \mu_{re} \frac{\partial H_z}{\partial t} + \frac{1}{r} \frac{\partial \left(r\rho\left(\frac{\partial H_r}{\partial z} - \frac{\partial H_z}{\partial r}\right)\right)}{\partial r} = 0 \end{cases} \tag{6}$$

3. Numerical results and discussions

3.1. Identical Ampere-turns (NIs) case

Fig. 5 shows the simulated AC loss results in SPCs with different horizontal gaps between the superconductor layers, g_h at 20 K plotted as a function of the coil current amplitude. The AC loss values decrease significantly with increasing g_h values. This should be due to the reduced superposition of the perpendicular magnetic field components with increasing g_h [36–39]. The difference in the loss values for different g_h values becomes smaller with increasing g_h. At $I_{t,\ coil} = 1000$ A, the AC loss values for $g_h = 0.1$ mm, 1 mm, and 2 mm, are 90 W, 43 W, and 28 W, respectively. At $I_{t,\ coil} = 2288$ A, the AC loss value for $g_h = 0.1$ mm is approximately-one order larger than that for $g_h = 2$ mm.

Table 2
REBCO wire specifications.

Wire type	REBCO
Manufacturer	SuperPower
Self-field I_c at 77 K (A)	457
Width (mm)	12
Thickness of superconductor layer (μm)	1.6
Hastelloy (μm)	50

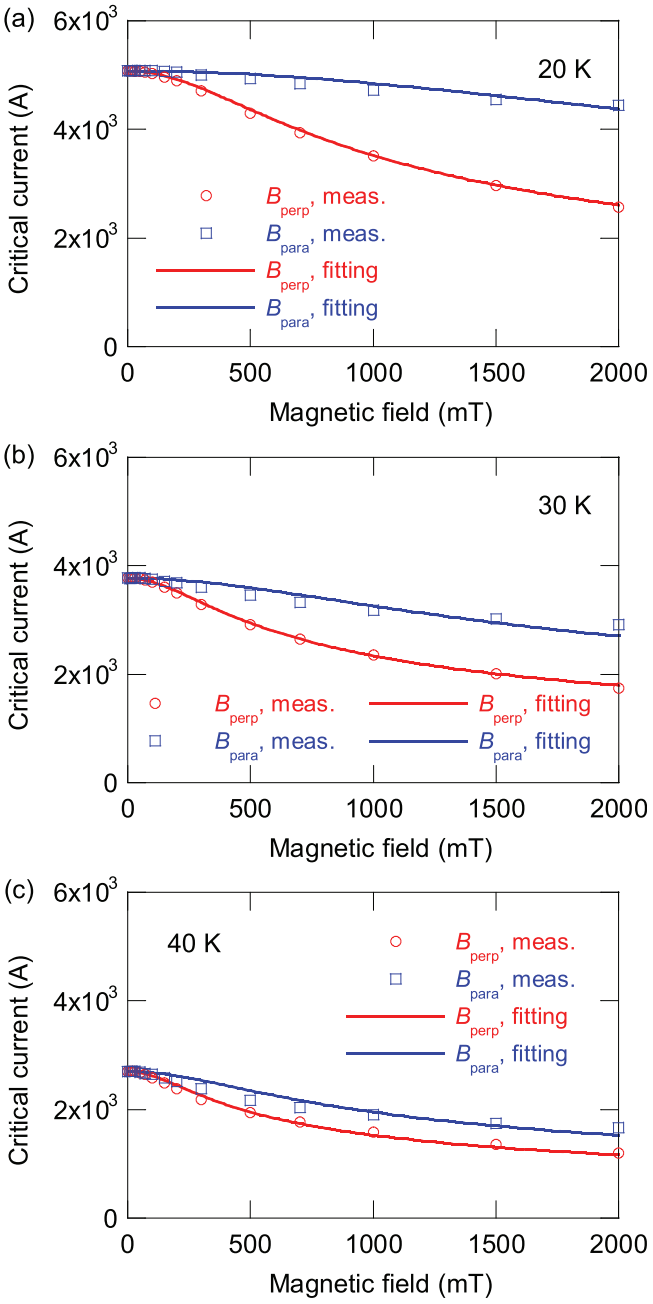

Fig. 4. The measured $I_c(B)$ results of the superconductor at different cryogenic temperatures. (a) 20 K, (b) 30 K, and (c) 40 K.

Table 3
REBCO wire specifications.

	20 K	30 K	40 K
Manufacturer			
Self-field I_c (A)	5084	3777	2706
B_0 (T)	0.55	0.32	0.25
k	0.045	0.33	0.5
α	0.25	0.2	0.2

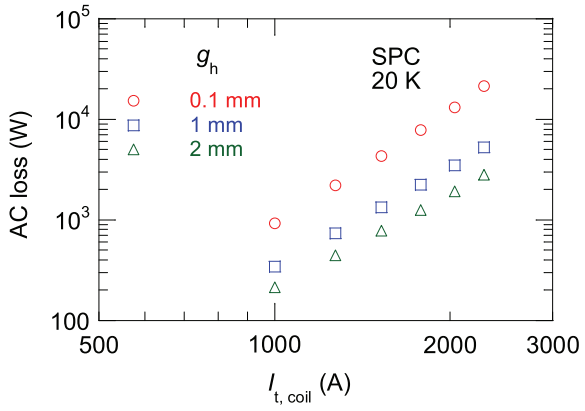

Fig. 5. Comparison of AC loss in single pancake coils (SPCs) with various g_h values 0.1, 1 and 2 mm at 20 K, 25 Hz.

In Fig. 6, the simulated AC loss results in 5PCs with different g_h values at 20 K are plotted as a function of the coil current amplitude. Interestingly, AC loss results for all different g_h values approximately agree with each other. Furthermore, the smallest g_h value leads to the smallest AC loss value - opposite to the results for SPCs shown in Fig. 5. The result can be explained by the magnetic field distribution of the 5PCs. In the 5PCs, only the end part of the coil windings is exposed to large perpendicular magnetic field component [25,40], and the center winding does not experience much perpendicular field component. When the perpendicular magnetic field component is smaller than the penetration field of the superconductor (see explanation for Fig. 9), the smaller the g_h the larger the shielding effect and hence the loss in this case is smaller than that with greater g_h [36].

Fig. 7 compares the simulated AC loss values between SPCs and 5PCs for the various g_h values shown in Figs. 5 and 6. The AC loss for SPC with g_h = 0.1 mm is much greater than all the 5PC results. For SPC with g_h = 2.0 mm the AC loss is much smaller than all the 5PC results. The AC loss for the 5PCs is slightly greater than that of SPC with g_h = 1 mm. This implies that spacing for SPC is more effective for AC loss reduction than having vertical structure for given Ampere-turns.

Fig. 8 compares the simulated AC loss values in the 5PC with g_h = 0.1 mm at various operating temperatures plotted as a function of the coil current amplitude. The AC loss in the 5PC increases with increasing the operating temperature. Fig. 9 compares the normalised current density, J/J_c of the 5PC at 20 K, 30 K, and 40 K. At all the operating temperatures, there is shielding current in all pancake coils except for the center pancake coil. Shielding current is the strongest

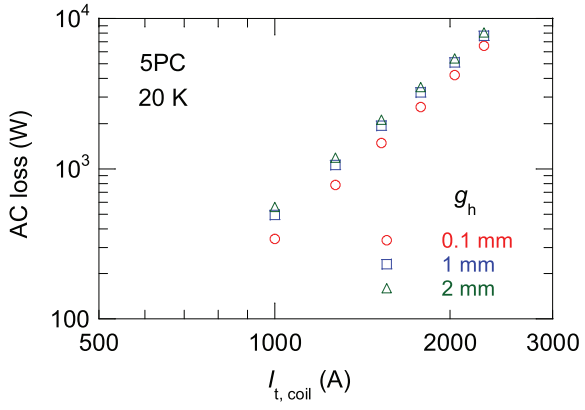

Fig. 6. Comparison of AC loss in stack of five pancake coils (5PCs) with various g_h values 0.1 mm, 1 mm, and 2 mm at 20 K, 25 Hz.

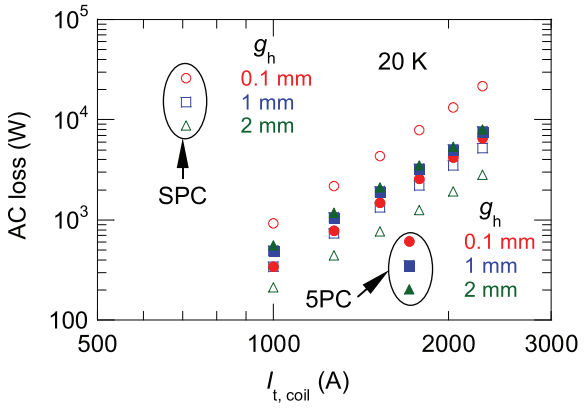

Fig. 7. Comparison of AC loss in SPCs and 5PCs with various g_h values 0.1 mm, 1 mm, and 2 mm at 20 K, 25 Hz.

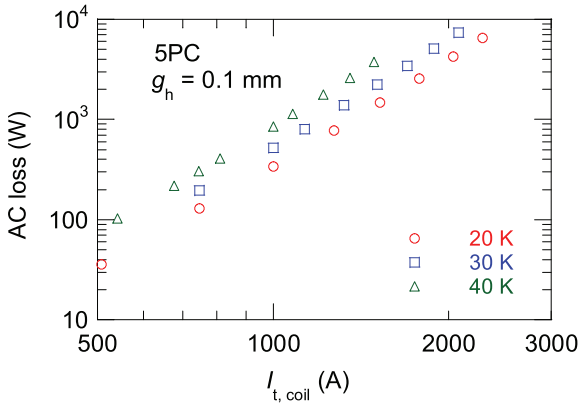

Fig. 8. AC loss dependence of 5PCs at 20 K, 30 K, and 40 K.

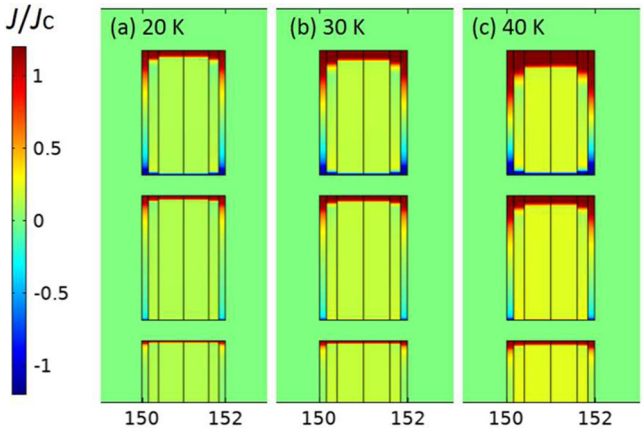

Fig. 9. Comparison of J/J_c distribution in the 5PCs when $I_{t, coil}$ = 747 A at 20 K, 30 K, and 40 K.

in the end pancake coil. In the 5PC the magnetic field distribution has the end pancake coils exposed to more perpendicular magnetic field component. Magnetic field penetration where $|J/J_c > 1|$ increases with increasing operating temperature as shown in Fig. 9. This is due to the temperature dependence of the I_c of the coated conductors used in the coil winding. When the operating temperature is increased the I_c of the coated conductor decreases and penetration magnetic field decreases because the penetration magnetic field is proportional to the I_c of the coated conductors [41,42]. Similar results

have been observed in the HTS armature windings at various operating temperatures under rotating magnetic fields [43]. The distribution of the normalized current densities explains the AC loss behaviours shown in Fig. 8 because the AC loss is mostly generated in the regions where $|J/J_c > 1|$ [30].

Fig. 10 compares AC loss values in the 5PC_HB coils (Fig. 1(b)) using different wires for the two end windings compared to the center winding at 20 K. The ratio of the self-field critical current I_c of the end windings to the self-field I_c of the center windings, $I_{c0,\,EW}/I_{c0,\,CW}$, varies between 0.6 to 2.0. The simulated AC loss results in the 5PC_HBs decrease with increasing $I_{c0,\,EW}/I_{c0,\,CW}$ values, which implies AC loss in the 5PC_HBs can be reduced by using the wires with higher I_c for the end windings. The reason can be explained by the higher I_c which makes magnetic field penetration more difficult.

Fig. 11 compares the simulated AC loss values in the 5PC_HB at 20 K and 1000 A for different $I_{c0,\,EW}/I_{c0,\,CW}$ values. The AC loss values drop sharply with increasing the ratio when the ratio is less than 1, while the decrease becomes more gradual when the ratio is greater than 1. Nevertheless, the AC loss is approximately halved for the ratio = 2 (at ~ 130 W) compared to that for the ratio = 1 (at ~ 260 W). The results clearly show the effectiveness of using high I_c wires for the end windings. As the curve tail becomes flat at ratio = 2, the optimal ratio is probably around 2, which seems feasible for practical application. Even at a ratio of 1.5, the AC loss reduction seems to be more than 50 %.

The simulated AC loss results in the SPCs with g_h = 0.1 mm and 2 mm with and without the flux diverters at 20 K are plotted as a function of the coil current amplitude in Fig. 12. The AC loss values in the SPCs for both horizontal gaps drop sharply with adding the FDs at the edges of the SPCs (at both edges and symmetrically about median plane). For instance, the AC loss in the SPC with g_h = 0.1 mm with the FDs at $I_{t,\,coil}$ = 1000 A, is less than 1/5 of the value without FDs. The difference between the AC loss results is greater with the smaller g_h. Adding the FDs is more effective at reducing AC loss in the coil with smaller g_h values.

Fig. 13 compares the magnetic field lines, and the distribution of the perpendicular magnetic field components, around the SPC for g_h = 0.1 mm with and without the FDs. It is clear that magnetic field around the HTS coil is more parallel in the SPC with the FD. The perpendicular field component near the edges of SPC with the FDs is much smaller than that of the SPC without the FDs because the high field concentration is diverted to the flux diverters. The results clearly show effectiveness of adding FDs in shaping the magnetic field near the REBCO coils [32]. The FDs will generate hysteresis and eddy current loss and the loss in the FDs could be large portion of the over-all loss (summation of the losses in the HTS windings and the flux diverters) generation of the HTS windings. Therefore, the losses in FDs need to be carefully evaluated, to assess the effectiveness of using FDs for AC loss reduction [27]. However, earlier work reported negligible loss in low-loss FDs using MPP (Molypermalloy powder) materials and high flux (HF) power materials attached to an HTS coil winding comprising of four stacked double pancake coils operating at 52.2 Hz [32,44,45]. It is worth noting that saturation of FDs at high coil current may weaken the effectiveness of FDs for AC loss reduction in the HTS coil windings [32].

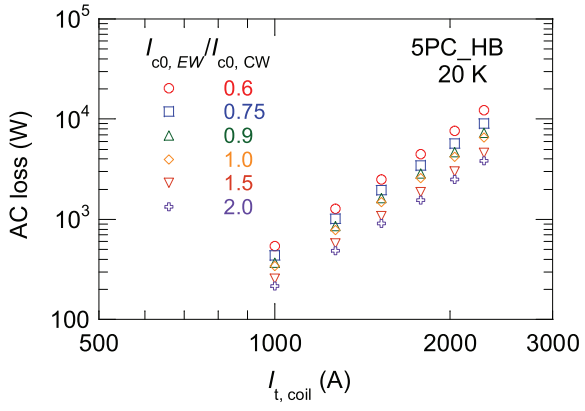

Fig. 10. Comparison of AC loss in 5PC, HBs (HB means hybrid) with various $(I_{c0,\,EW})/(I_{c0,\,CW})$, when horizontal gap g_h = 0.1 mm at 20 K, 25 Hz. The EW is for end winding, and CW is for center winding.

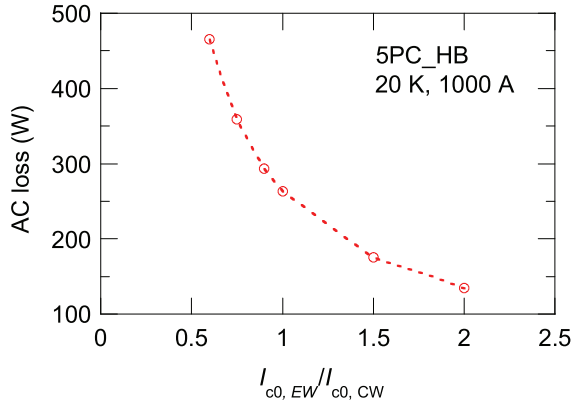

Fig. 11. AC loss dependence of 5PC, HBs on $I_{c0,\,EW}/I_{c0,\,CW}$ values when $I_{t,\,coil}$ = 1000 A, at 20 K, 25 Hz.

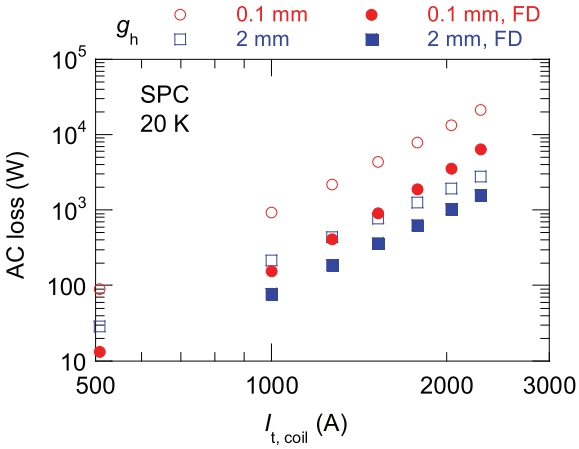

Fig. 12. Comparison of AC loss values in SPCs with and without flux diverters. FD stands for flux diverters.

In Fig. 14, the simulated AC loss results in the 5PC_HBs for $I_{c0,\,EW}/I_{c0,\,CW}$ = 1.0 and 2.0 without FDs, and in the 5PC for $I_{c0,\,EW}/I_{c0,\,CW}$ = 1.0 with FDs are plotted as a function of the coil current amplitude. The AC loss values in the 5PC_ HB for $I_{c0,\,EW}/I_{c0,\,CW}$ = 1.0 with FDs are substantially smaller than those in the 5PC_HB for $I_{c0,\,EW}/I_{c0,\,CW}$ = 2.0 without FDs. The results imply utilizing FDs are more effective than grading I_c in the coil windings for reducing AC loss.

Fig. 15 presents the magnetic field flux lines and the distribution of the perpendicular magnetic field components around the 5PC with and without the FDs. Like the case for SPCs, the magnetic field becomes more parallel with the flux diverters and the perpendicular magnetic field component at the edges of each pancake coil is significantly reduced by using FDs.

Fig. 16 compares the simulated AC loss values in the SPCs with g_h = 0.1 mm and 2 mm with FDs, and in the 5PC with g_h = 0.1 mm with FDs at 20 K. The AC loss in the SPC with g_h = 2 mm with FDs is much smaller than that with g_h = 0.1 mm. At I_t = 1000 A, the AC loss

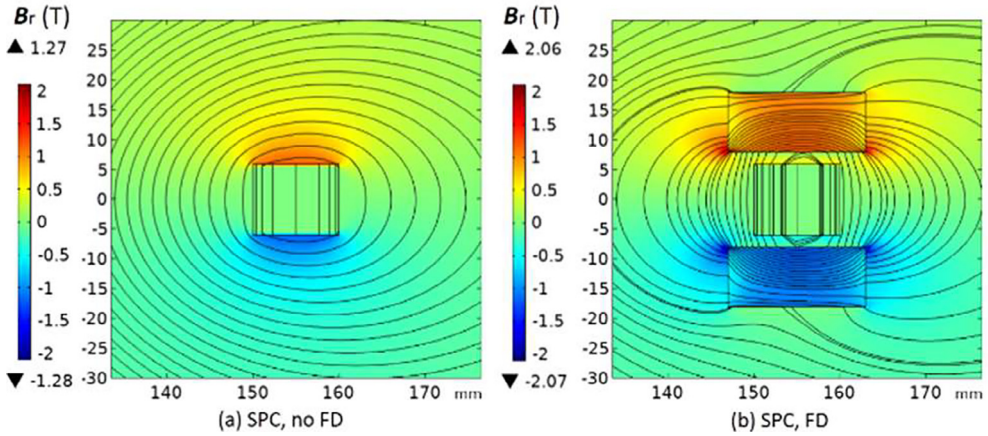

Fig. 13. Comparison of Br contribution in the SPCs without (left) and with (right) flux diverters when $I_{t,\ coil}$ = 1000 A.

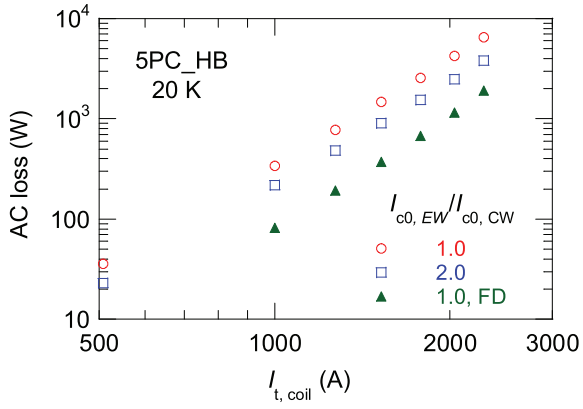

Fig. 14. Comparison of AC loss values in the 5PC_HB with and without FDs at 20 K.

for the SPC with g_h = 2 mm is approximately 77 W, smaller than 154 W for the SPC with g_h = 0.1 mm. However, it should be noted that the FDs for the SPC with g_h = 2 mm are much wider than those of the SPC with g_h = 0.1 mm. The AC loss values in the 5PC for g_h = 0.1 mm with the FDs agree well with those in the SPC for g_h = 2 mm with the FDs.

3.2. Comparison of magnetic field distributions in coils

Comparing coil configurations with a view to reduce the AC loss in the winding pack, the field at the center point was targeted at 0.15 T for fair comparison. The magnetic field for various configurations mentioned above was checked and compared as shown in the following plots.

In the SPC configuration shown in Fig. 17, the horizontal gap between turns varies from 0.1, to 1 and 2 mm. The coil height is 12 mm, and its half is 6 mm. The magnetic field B_z component along the magnet axis decreases as the distance from the center increases. The larger the gap, the larger the coil OD, the least rate of field decrease.

Magnetic field B_z in the SPCs with or without FDs are compared in Fig. 18. Typical magnetic flux contours without and with FDs are displayed in Fig. 19. Although the FDs change the flux direction near the coil edge considerably, only small effects on the magnetic field along coil axis are seen, which is an advantage for practical magnet design; this indicates that reducing coil AC loss with FDs does not reduce the magnet bore field.

In the case of 5PCs shown in Fig. 20, the total coil height is about 5 times that of SPCs, yet magnetic field along the magnet axis exhibits only small reduction within the coil height as indicated by the blue box. Increasing the horizontal turn gaps from 0.1 mm to 2 mm, causes little difference for the magnetic field at 40 mm and beyond. This

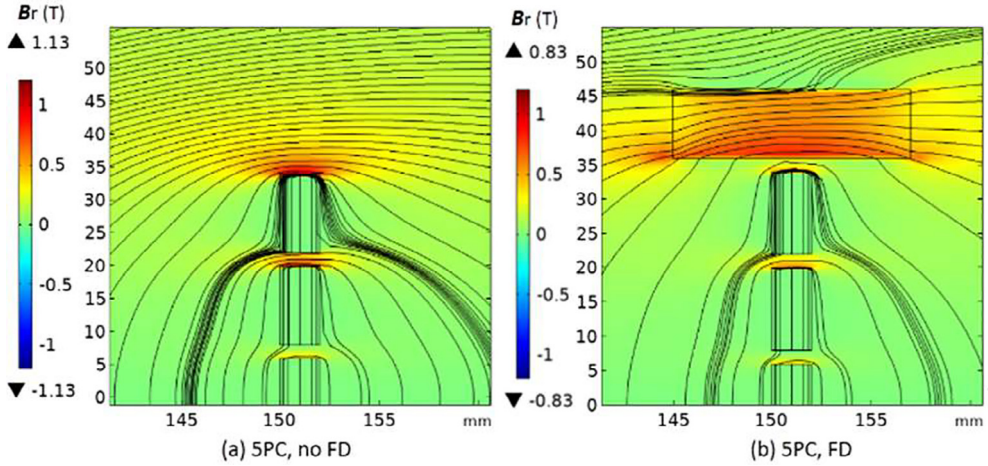

Fig. 15. Comparison of B_r contribution in the 5PCs without (left) and with (right) flux diverters when $I_{t,\ coil}$ = 1000 A, g_h = 0.1 mm at 20 K, 25 Hz.

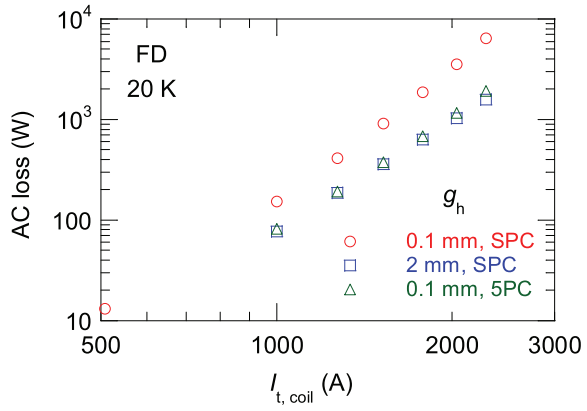

Fig. 16. Comparison of AC loss values in SPCs with g_h = 0.1 mm and 2 mm, and the 5PC with g_h = 0.1 mm with the flux diverters at 20 K.

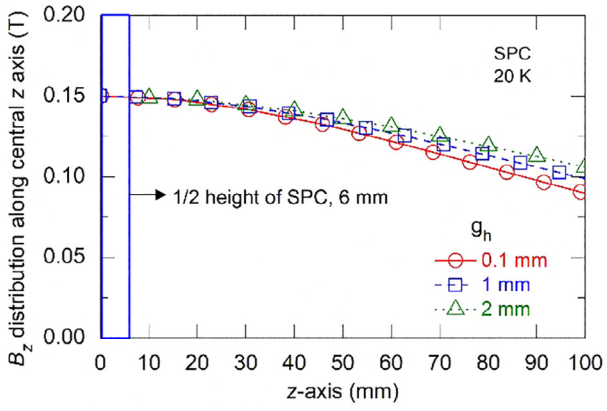

Fig. 17. Comparison of B_z distribution along the coil center axis in the SPCs when B (0, 0) = 0.15 T. B (0, 0) stands for the magnetic field at center point (0, 0).

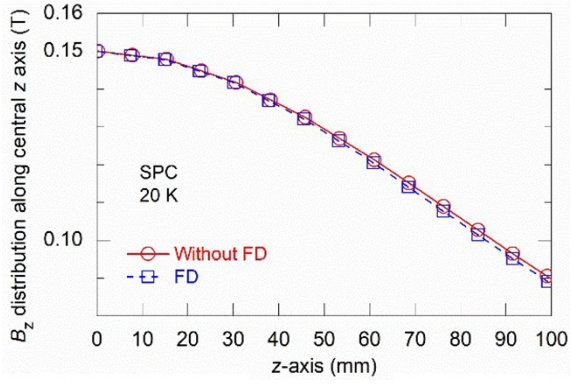

Fig. 18. Comparison of B_z distribution along the coil center axis in the SPCs with without FDs when B (0, 0) = 0.15 T and g_h = 0.1 mm. B (0, 0) stands for the magnetic field at center point (0, 0).

allows flexibility in adjusting turn-to-turn gaps in large scale multiple coil design.

For 5PCs without or with FDs shown in Fig. 21, there is only small variations in the center field for the two cases similar to the cases for SPCs shown in Fig. 18. Adding FDs is an effective method in reducing the coil AC loss while maintaining effective center magnetic field.

3.3. AC loss comparison in HTS coils for the same center field

The magnet designs mentioned above generate slightly different magnetic field even though they have same Ampere-turns due to their different geometries. In the following, we compare the AC loss in the coils when they generate the same magnetic field in the center of the coils. It is worth noting that the relationship between the magnetic field at the coil center and the coil current is linear.

Fig. 22 compares the AC loss results in the SPCs at 20 K for different g_h values plotted as a function of the center magnetic field. Although the AC loss values decrease with increasing g_h values, the difference between the AC loss values becomes much smaller compared to the case where Ampere-turns are the same shown in Fig. 5. Since the field constant becomes smaller with increasing g_h values, and hence more Ampere-turns are needed for larger turn-to-turn gaps. The AC loss values for g_h = 1 mm and 2 mm are almost the same.

Fig. 23 compares the simulated AC loss results in the 5PCs at 20 K for different g_h values plotted as a function of the center magnetic field. Compared to the case for the same Ampere-turns shown in Fig. 6, the AC loss values for g_h = 0.1 mm become much smaller than the values for the other two horizontal gaps. It is obvious that keeping small horizontal gaps is beneficial both for reducing AC loss and increasing efficiency of magnetic field generation in the 5PCs configurations, particularly for solenoid type coils.

In Fig. 24, the simulated AC loss results in the SPC with g_h = 2 mm and the 5PC with g_h = 0.1 mm are plotted as a function of a function of the center magnetic field. The significant difference between the two cases when plotted against the same Ampere-turns shown in Fig. 7 disappears completely. This is understandable considering the reduced field constant with larger turn-to-turn gaps, particularly for higher field > 0.2 T.

Fig. 25 compares the simulated AC loss results in the SPCs with g_h = 0.1 mm and 2 mm without and with the FDs at both edges of the coils plotted as a function of the center magnetic field. The AC loss values in the SPC with g_h = 2 mm are still much smaller than those in the SPC with g_h = 0.1 mm. However, the difference between the two coils with the FDs vanishes almost completely. It is worth noting that the size of the FDs in the case of g_h = 2 mm is much greater than that of g_h = 0.1 mm. The result implies that spacing is not effective when FDs are used for SPCs considering both the center magnetic field and AC loss reduction.

In Fig. 26, the simulated AC loss results in the SPC and 5PC with g_h = 0.1 mm with FDs at the top and bottom edges of the coils are plotted as a function of the center magnetic field. Throughout the center magnetic fields, the AC loss in the 5PCs is much less than that of the SPC and the difference becomes greater with increasing the center magnetic field. The result clearly indicates that solenoid type coil configuration with FDs offers distinctive advantage over the single pancake type with FDs when considering both field generation capability and AC loss reduction.

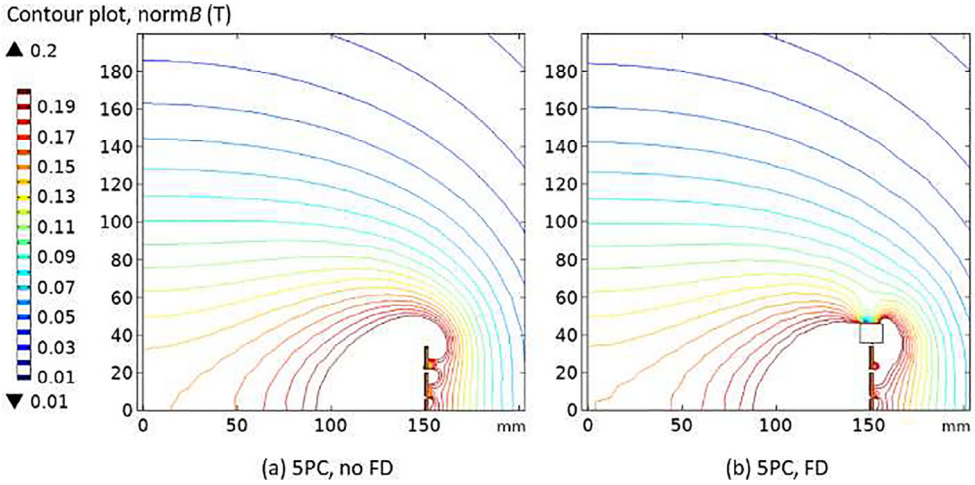

Fig. 19. Magnetic field contour plots for SPCs with and without flux diverters.

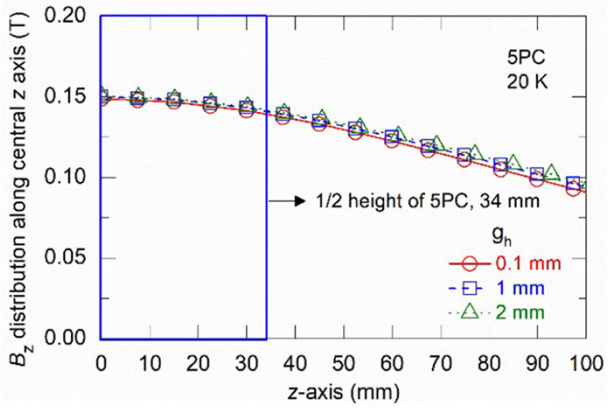

Fig. 20. Comparison of B_z distribution along the coil center axis in the 5PCs when B (0, 0) = 0.15 T. B (0, 0) stands for the magnetic field at center point (0, 0).

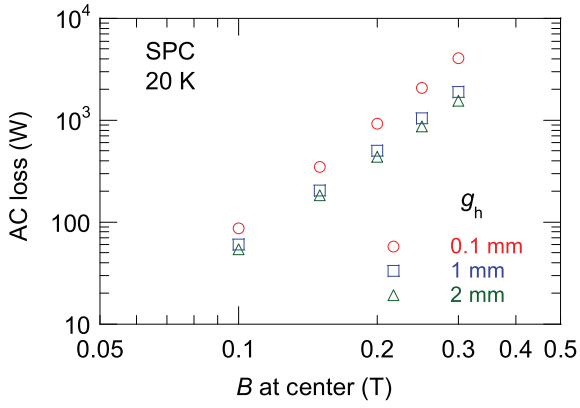

Fig. 22. AC loss comparison in SPCs with various g_h values at 20 K, 25 Hz.

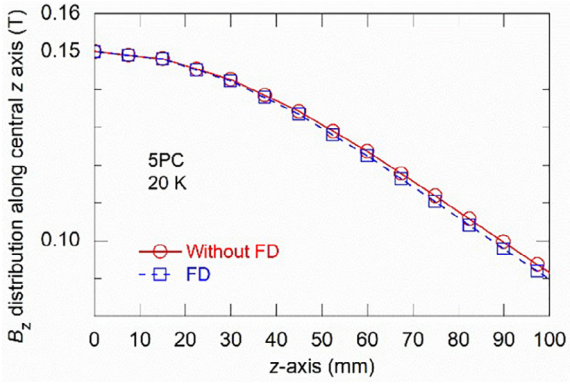

Fig. 21. Comparison of B_z distribution along the coil center axis in the 5PCs with and without FDs when g_h = 0.1 mm and B (0, 0) = 0.15 T. B (0, 0) stands for the magnetic field at center point (0, 0).

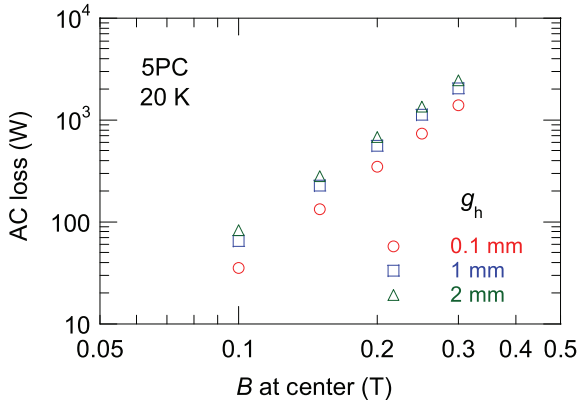

Fig. 23. AC loss comparison in 5PCs with various g_h values at 20 K, 25 Hz when B (0, 0) = 0.15 T.

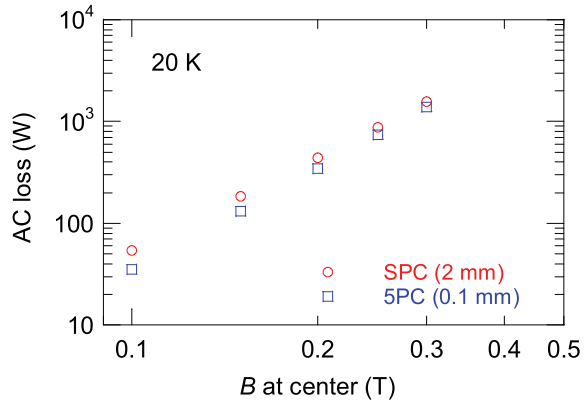

Fig. 24. Comparison of AC loss in the SPC with g_h = 2 mm and the 5PCs with g_h = 0.1 mm at 20 K, 25 Hz when B (0, 0) = 0.15 T.

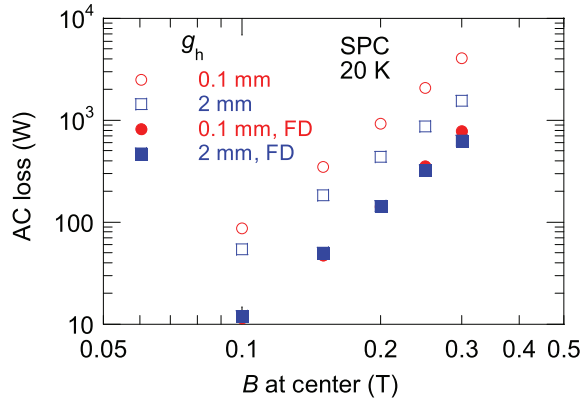

Fig. 25. Comparison of AC loss in SPCs with g_h = 0.1 mm and 2 mm with and without FDs at 20 K, 25 Hz when B (0, 0) = 0.15 T.

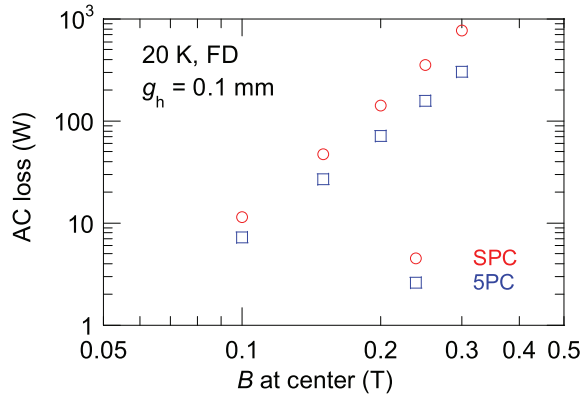

Fig. 26. Comparison of AC loss in the SPC and 5PC with g_h = 0.1 mm with flux diverters at 20 K, 25 Hz when B (0, 0) = 0.15 T.

4. Conclusions

In this work, we numerically studied coil configurations of several small superconducting magnets, constructed from 12 mm SuperPower REBCO coated conductors, for fast-ramping application with the same Ampere-turns to identify the lowest AC loss. We incorporated existing loss reduction strategies including spacing between the turns for SPCs, grading I_c values for solenoid configuration, and applying flux diverters to shape the magnetic field around the coil windings. The simulation was implemented using a homogenized H-formulation.

It was found that spacing is enormously effective for reducing AC loss for SPCs. The difference between the AC loss values for g_h = 0.1-mm and 2 mm at $I_{c,\ coil}$ = 2288 A is approximately-one order of magnitude.

For 5PCs, the AC loss values in 5PCs decrease with decreasing the horizontal gaps which is the opposite to the tendency seen in the SPCs although the difference between the loss values for different g_h values are small. In 5PCs, the AC loss is dominated by the magnetization loss in the end windings due to the perpendicular magnetic field component and the smaller g_h the larger the shielding effect and hence the loss in this situation is smaller than that with greater g_h.

Grading I_c values for 5PCs, i.e., using high I_c wires for the end windings of 5PCs is effective for reducing AC loss in the coils although it also shows saturation when $I_{c0,\ EW}/I_{c0,\ CW} > 2$. The results can be explained by the weakened magnetic field penetration into the end windings by using high I_c wires. AC loss in the 5PC increases with increasing operating temperature. This is due to increase of magnetic field penetration into the coil windings due to decrease of I_c in the HTS conductors.

Across all studied loss reduction methods, the use of flux diverters has the largest impact in AC loss reduction. The AC loss values in the 5PC for g_h = 0.1 mm with the flux diverters agree well with those in the SPC for g_h = 2 mm with the flux diverters. However, the loss reduction effect might be reduced at high operating current due to the saturation of the flux diverters. It is important to note that adding flux diverters does not affect the center field.

Spacing for SPCs rapidly loses advantage for both with and without the flux diverters in reducing AC loss when the coil AC losses are compared as a function of the center magnetic field. This should be due to the reduced capability of generating magnetic field due to spacing. More Ampere-turns is needed to maintain the same center field for larger turn gaps.

Solenoid type coil configurations with flux diverters offers distinctive advantage over the single pancake type with flux diverters from the viewpoint of both field generation capability and low AC loss and hence is the best option for this study. The simulation results in this work have practical implications for fast-ramping design.

Declaration of Competing Interest

The authors declare that they have no known competing financial interests or personal relationships that could have appeared to influence the work reported in this paper.

Acknowledgement

This work was supported in part by New Zealand Ministry of Business, Innovation and Employment (MBIE) by the Strategic Science Investment Fund "Advanced Energy Technology Platforms" under Contract RTVU2004. H. Song would like to thank for the following funding support: 2020 Google Excellence Research University Program; US DOE Ernst Courant Traineeship in Accelerator Sciences and Engineering, the educational program of next generation of accelerator physicists and engineer, US Department of Energy, HEP office.

References

[1] Schmidt W, Gamble B, Kraemer H-P, Madura D, Otto A, Romanosky W. Design and test of current limiting modules using YBCO-coated conductors. Supercond Sci Technol 2010;23(1):014024.

[2] Iwakuma M, Sakaki K, Tomioka A, Miyayama T, Konno M, Hayashi H, et al. Development of a 3ϕ-66/6.9 kV-2 MVA REBCO superconducting transformer. IEEE Trans Appl Supercond 2015;25(3):1–6, 5500206. https://doi.org/10.1109/TASC.2014.2364615.

[3] Honghai Song, Brownsey P, Yifei Zhang, Waterman J, Fukushima T, Hazelton D. 2G HTS coil technology development at SuperPower. IEEE Trans Appl Supercond 2013;23(3):4600806.

[4] Hahn S, Kim K, Kim K, Hu X, Painter T, Dixon I, et al. 45.5-tesla direct-current magnetic field generated with a high-temperature superconducting magnet. Nature 2019;570(7762):496–9.

[5] Schwartz J, Effio T, Xiaotao Liu, Le QV, Mbaruku AL, Schneider-Muntau HJ, et al. High field superconducting solenoids via high temperature superconductors. IEEE Trans Appl Supercond 2008;18(2):70–81.

[6] Song H, Burkhardt EE, Borden T, Chouhan S, Cole D, Georgobiani D, et al. Design and engineering of an HTS dipole in the FRIB fragment separator. IEEE Trans Appl Supercond 2015;25(3):1–6, 4602506. https://doi.org/10.1109/TASC.2014.2374602.

[7] Song H, Hazelton D, Fukushima D, Brownsey P. Engineering design and novel winding approaches in developing high quality HTS REBCO coils. IEEE Trans Appl Supercond 2017;27(4):1–5.

[8] Song H. Sudden-discharge cycling characteristics and millisecond dynamic behaviors of a HTS stainless-steel insulated double-pancake coil with thin copper plates. IEEE Trans Appl Supercond 2020;30(4):1–6, 4702506. https://doi.org/10.1109/TASC.2020.2975770.

[9] Guo Z, Qin J, Lubkemann R, Wang K, Jin H, Xiao G, et al. AC loss and contact resistance in highly flexible rebco cable for fusion applications. Superconductivity 2022;2:100013.

[10] Yagotintsev K, Anvar VA, Gao P, Dhalle MJ, Haugan TJ, Van Der Laan DC, et al. AC loss and contact resistance in REBCO CORC®, Roebel, and stacked tape cables. Supercond Sci Technol 2020;33(8):085009.

[11] Song HH, Gagnon K, Schwartz J. Quench behavior of conduction-cooled YBa2Cu3O7-delta coated conductor pancake coils stabilized with brass or copper. Supercond Sci Technol 2010;23(6).

[12] Kramer D. Helium shortage has ended, at least for now 2020.

[13] Kramer D. Helium is again in short supply 2022.

[14] Piekarz H, Hays S, Blowers J, Claypool B, Shiltsev V. Record fast-cycling accelerator magnet based on HTS conductor. Nucl Instrum Methods Phys Res, Sect A 2019;943:162490.

[15] Piekarz H, Hays S, Claypool B, Kufer M, Shiltsev V. Record high ramping rates in HTS based superconducting accelerator magnet. IEEE Trans Appl Supercond 2022;32(6):1–4, 4100404. https://doi.org/10.1109/TASC.2022.3151047.

[16] Single-Stage Pulse Tube Cryocoolers 2022 [Available from: https://www.cryomech.com/cryocoolers/pulse-tube-cryocoolers/#single-stage.

[17] Amemiya N, Kasai S, Yoda K, Jiang Z, Levin GA, Barnes PN, et al. AC loss reduction of YBCO coated conductors by multifilamentary structure. Supercond Sci Technol 2004;17(12):1464–71.

[18] Long NJ, Badcock RA, Hamilton K, Wright A, Jiang Z, Lakshmi LS. Development of YBCO Roebel cables for high current transport and low AC loss applications. J Phys Conf Ser 2010;234(2):022021.

[19] Jiang Z, Komeda T, Amemiya N, Long NJ, Staines M, Badcock RA, et al. Total AC loss measurements in a six strand Roebel cable carrying an AC current in an AC magnetic field. Supercond Sci Technol 2013;26(3):035014.

[20] van der Laan DC, Weiss JD, McRae DM. Status of CORC (R) cables and wires for use in high-field magnets and power systems a decade after their introduction. Supercond Sci Technol 2019;32(3), 033001:. https://doi.org/10.1088/1361-6668/aafc82.

[21] van der Laan DC, Lu XF, Goodrich LF. Compact GdBaCuO coated conductor cables for electric power transmission and magnet applications. Supercond Sci Technol 2011;24(4):042001.

[22] Vojenčiak M, Kario A, Ringsdorf B, Nast R, van der Laan DC, Scheiter J, et al. Magnetization ac loss reduction in HTS CORC cables made of striated coated conductors. Supercond Sci Technol 2015;28(10):104006.

[23] Amemiya N, Shigemasa M, Takahashi A, Wang N, Sogabe Y, Yamano S, et al. Effective reduction of magnetisation losses in copper-plated multifilament coated conductors using spiral geometry. Supercond Sci Technol 2022;35(2):025003.

[24] Jiang Z, Long NJ, Badcock RA, Staines M, Slade RA, Caplin AD, et al. AC loss measurements in pancake coils wound with 2G tapes and Roebel cable: dependence on spacing between turns/strands. Supercond Sci Technol 2012;25(3):035002.

[25] Jiang Z, Long NJ, Staines M, Badcock RA, Bumby CW, Buckley RG, et al. AC loss measurements in HTS coil assemblies with hybrid coil structures. Supercond Sci Technol 2016;29(9):095011.

[26] Song W, Jiang Z, Staines M, Wimbush S, Badcock R, Fang J. AC loss calculation on a 6.5 MVA/25 kV HTS traction transformer with hybrid winding structure. IEEE Trans Appl Supercond 2020;30(4):1–5 5500405. https://doi.org/10.1109/TASC.2020.2975771.

[27] Pardo E, Šouc J, Vojenčiak M. AC loss measurement and simulation of a coated conductor pancake coil with ferromagnetic parts. Supercond Sci Technol 2009;22(7):075007.

[28] Ainslie MD, Weijia Yuan, Flack TJ. Numerical analysis of AC loss reduction in HTS superconducting coils using magnetic materials to divert flux. IEEE Trans Appl Supercond 2013;23(3):4700104.

[29] Liu G, Zhang G, Jing L, Yu H. Numerical study on AC loss reduction of stacked HTS tapes by optimal design of flux diverter. Supercond Sci Technol 2017;30(12):125014.

[30] Song W, Jiang Z, Staines M, Badcock RA, Wimbush SC, Fang J, et al. Design of a single-phase 6.5 MVA/25 kV superconducting traction transformer for the Chinese Fuxing high-speed train. Int J Electr Power Energy Syst 2020;119:105956.

[31] You S, Staines M, Sidorov G, Miyagi D, Badcock RA, Long NJ, et al. AC loss measurement and simulation in a REBCO coil assembly utilising low-loss magnetic flux diverters. Supercond Sci Technol 2020;33(11):115011.

[32] You S, Miyagi D, Badcock RA, Long NJ, Jiang Z. Experimental and numerical study on AC loss reduction in a REBCO coil assembly by applying high saturation field powder-core flux diverters. Cryogenics 2022;124:103466.

[33] Hong Z, Campbell AM, Coombs TA. Numerical solution of critical state in superconductivity by finite element software. Supercond Sci Technol 2006;19(12):1246–52.

[34] Zermeno VMR, Abrahamsen AB, Mijatovic N, Jensen BB, Sørensen MP. Calculation of alternating current losses in stacks and coils made of second generation high temperature superconducting tapes for large scale applications. J Appl Phys 2013;114(17):173901.

[35] Song W, Jiang Z, Zhang X, Staines M, Badcock RA, Fang J, et al. AC loss simulation in a HTS 3-Phase 1 MVA transformer using H formulation. Cryogenics 2018;94:14–21.

[36] Jiang Z, Amemiya N, Kakimoto K, Iijima Y, Saitoh T, Shiohara Y. The dependence of AC loss characteristics on the space in stacked YBCO conductors. Supercond Sci Technol 2008;21(1):015020.

[37] Jiang Z, Thakur KP, Staines M, Badcock RA, Long NJ, Buckley RG, et al. The dependence of AC loss characteristics on the spacing between strands in YBCO Roebel cables. Supercond Sci Technol 2011;24(6):065005.

[38] Šouc J, Gömöry F, Vojenčiak M. Coated conductor arrangement for reduced AC losses in a resistive-type superconducting fault current limiter. Supercond Sci Technol 2012;25(1):014005.

[39] Song W, Jiang Z, Zhang X, Staines M, Bumby CW, Badcock RA, et al. Transport AC loss measurements in bifilar stacks composed of YBCO-coated conductors. IEEE Trans Appl Supercond 2018;28(4):1–6.

[40] Jiang Z, Song W, Pei X, Fang J, Badcock RA, Wimbush SC. 15% reduction in AC loss of a 3-phase 1 MVA HTS transformer by exploiting asymmetric conductor critical current. J Phys Commun 2021;5(2):025003.

[41] Jiang Z, Toyomoto R, Amemiya N, Zhang X, Bumby CW. Dynamic resistance of a high-T_c coated conductor wire in a perpendicular magnetic field at 77 K. Supercond Sci Technol 2017;30(3):03LT01.

[42] Brandt EH, Indenbom M. Type-II-superconductor strip with current in a perpendicular magnetic field. Physical Review B 1993;48(17):12893–906.

[43] You S, Kalsi SS, Ainslie MD, Badcock RA, Long NJ, Jiang Z. Simulation of AC loss in the armature windings of a 100 kW all-HTS motor with various (RE)BCO conductor considerations. IEEE Access 2021;9:130968–80.

[44] https://www.mag-inc.com/Products/Powder-Cores/MPP-Cores/Learn-More-about-MPP-Core.

[45] https://www. mag-inc.com/Products/Powder-Cores/High-Flux-Cores/Learn-More-about-High -Flux-Cores.